JOURNAL DE PHYSIQUE IV
Colloque C4, supplément au Journal de Physique III, Volume 4, avril 1994

Laser plasma formation in metals vapour: kinetic approach

V. MAZHUKIN, I. GUSEV, I. SMUROV* and G. FLAMANT**

Institute of Mathematical Modeling, Russian Academy of Sciences, Miusskaya Square 4, 125047 Moscow, Russia
** Ecole Nationale d'Ingénieurs de Saint-Etienne, 58 rue Jean Parot, 42023 Saint-Etienne cedex 2, France*
*** Institut de Science et de Génie des Matériaux et Procédés, CNRS, BP. 5, Odeillo, 66125 Font-Romeu cedex, France*

ABSTRACT

The break-down of metals vapour (Al, Cu) are simulated near the break-down threshold values of laser radiation. The approximations of collision-radiation model are used, including the detail kinetics of exited states with radiation and collision transitions, step-by-step ionisation process, unexitation and recombination. Energy balance is based on two-temperature approximation : for electrons and for heavy particles. It is shown that the particles concentration in exited states and plasma species composition differ rather from Saha-Boltzmann's distribution. Strong dependence of the break-down threshold intensity on initial temperature of neutral and charged particles is shown.

1. Basis of Physical and Mathematical Model

It is assumed that the metal vapours passing through the Knudsen's layer are initially in the equilibrium state, i.e. initial concentration of atoms and ions in the ground and in the excited states are determined by the Saha-Boltzmann's equations.

The main elementary processes taken into account by the collisional-radiational model are as follows :

. Spontaneous radiative decay of excited states

$$A^z_n \xrightarrow{a^z_{nm}} A^z_m + h\omega$$

where a^z_{mn} $[s^{-1}]$ is the rate constant for radiation transition from n-state to m-state $h\omega$ - released quantum.

. Excitation and un excitation of atoms and ions by electron collision

$$A^z_n + e \xleftrightarrow{k^z_{mn},\,k^z_{nm}} A^z_m + e$$

where k^z_{mn} $[cm^3 . s^{-1}]$ is electron-particle reaction rate constant for z-charged particle excitation from state m to state n; k^z_{nm} - unexcitation rate constant for the n - th level.

. Ionization of the ground and excited states of atoms and ions by electron impact

$$A^z_n + e \xrightarrow{\alpha^z_n} A^z_o{}^{+1} + e + e$$

where α^z_n [$cm^3.s^{-1}$] is electron-particle reaction rate constant for the n-th level ionization of z-charged particle.

. Reaction reversible to the collision ionization : three particles recombination (the third particle is an electron)

$$A_o^{z+1} + e + e \xrightarrow{\beta^z_n} A^z_n + e$$

where β^z_n [$cm^6.s^{-1}$] is reaction rate constant.

For example, we have listed in table 1 the various energy levels take into account in the model for aluminium species.[1]

Table 1 : Energy levels of Al neutral atom Al^*, Al^{2+} ions used in the model.

N^o	Al	Al^{1+}	Al^{2+}
1	$1s^22s^22p^63s^23p$ $(^2P^o)$	$1s^22s^22p^63s^2$ (^1S)	$1s^22s^22p^63s$ (^2S)
2	$4s$ (^2S)	$3s3p$ $(^{1,3}P^o)$	$3p$ $(^2P^o)$
3	$3d$ (^2D)	$3s4s$ $(^{1,3}S)$	$3d$ $(^2P^o)$
4	$4p$ $(^2P^o)$	$3s3d$ $(^{1,3})$	$4s$ (^2S)
5	$5s$ (^2S)	$3s4p$ $(^{1,3}P^o)$	$4p$ $(^2P^o)$
6	$4d$ (^2D)	$3s4d$ $(^{1,3}D)$	$4d$ (^2D)
7	$5p$ $(^2P^o)$	$3s6$	$4f$ (^2D)
8	$4f$ $(^2F^o)$	$3s7$	$5s$ (^2S)
9	$6s,p$ $(^2S,^2P^o)$	$3s8$	$5p$ $(^2P^o)$
10	$5d$ $(^2D^o)$		$5f$ (^2F)
11	$6f$ $(^2F^o)$		$2p^67$
12	$6d,f$ $(^2D,^2F^o)$		$2p^68$
13	$3s^27 - 3s^210$		$2p^69$

On this basis, the distribution of ions and level-to-level kinetics of neutral atoms and ions is calculated by a system of nnon linear differential equations [2].

2. Results and Discussion

The values of laser intensity used in the simulation correspond the near break-down threshold values (λ=1.06 µm, G=10^6 + 10^9 W/cm^2 for Al, G=10^6 + 10^{10} W/cm^2 for Cu). The initial values of vapour temperature T^o and density ΣN^z_n are equal for both metals and correspond to the Knudsen's layer values during intensive evaporation : T^o=0.2 eV, $\Sigma N^z_n = 6.10^{18}$ cm^{-3},
Two typical regimes are considered :

. Laser intensity is below the threshold values of avalanche-like ionization (G<10^9 W/cm^2 for Al, G<2.10^8 W/cm^2 for Cu);

. Optical break-down development when a partially ionized gas transforms into a fully ionized plasma.

The transition between both situations is illustrated in Fig.1.

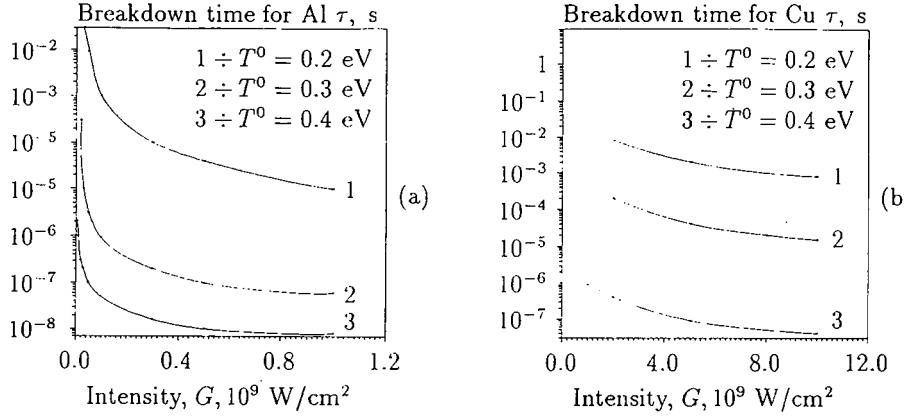

Figure 1 : The dependence of breakdown period for Al (a) and Cu (b) versus laser radiation intensity G for different values of initial temperature T^o.

The dynamics of the process is illustrated in Figures 2-7.

If intensity of the laser radiation is below the threshold value (as illustrated in Figures 2-5) metal vapour passes from the initial equilibrium state through the transient stage of nonequilibrium processes to another equilibrium steady state, which differs rather from Saha-Boltzmann's distribution. The quantitative estimates of new distribution do not coincide with the Saha-Boltzmann ones because of a powerful spontaneous radiation. Thereby the Saha-Boltzmann description turns out to be inadequate to describe optical characteristics of the laser flame.

For laser intensity larger than the threshold value, Figure 6 and 7 related to Al and Cu vapours respectively show that the optical break down is essentially a non equilibrium transition phenomenon from a partially ionized vapour to a completely ionized plasma. The characteristic time of the transition varies with the composition of the vapour.

3. CONCLUSION

This model described the time dependance of concentration and temperature of electron and heavy particles during the interaction of laser radiation with metallic vapour. It is shown that : The transitions are essentially non equilibrium processes

- The optical breakdown threshold depends strongly on vapour composition

REFERENCES

[1] MOORE Ch.E., (1971), Atomic Energy levels, NBS Washington, Vol.1.

[2] MAZHUKIN V.F., GUSEW I.V., SMUROV I., FLAMANT G. "Analysis of non equilibrium phenomena during interaction of laser radiation with metal vapours", submitted to Plasma Physics, (1994).

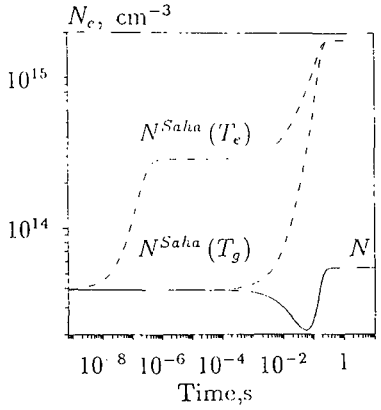

Figure 2: Concentration of charged particles ($N_e \sim \sum_{i,z} N_i^z$) in Al vapour ($G = 10^7$ W/cm^2). Dashed curves: equilibrium concentration of charged particles (based on Saha equations) for T_e, T_g temperatures.

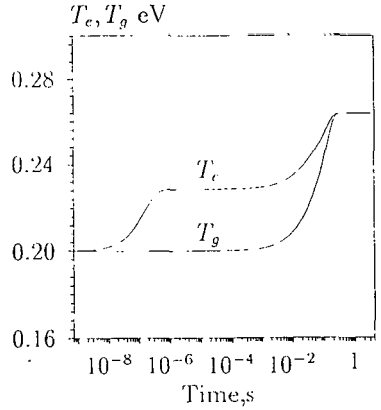

Figure 3: Temperature of electrons T_e and heavy particles (atoms, ions) in Al vapour ($G = 10^7$ W/cm^2).

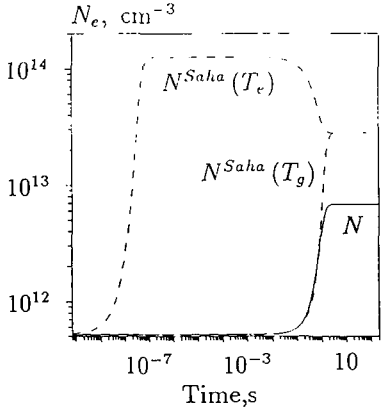

Figure 4: Concentration of charged particles ($N_e \sim \sum_{i,z} N_i^z$ in Cu vapour ($G = 10^8$ W/cm^2). Dashed curves: equilibrium concentration of charged particles (based on Saha equations) for T_e, T_g temperatures.

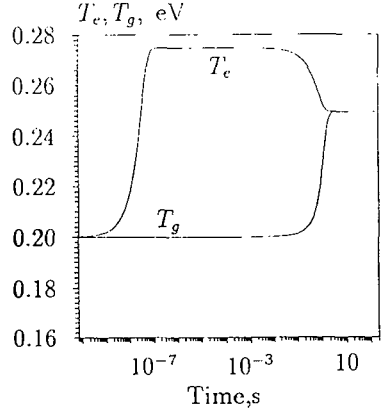

Figure 5: Temperature of electrons T_e and heavy particles (atoms, ions) in Cu vapour ($G = 10^8$ W/cm^2).

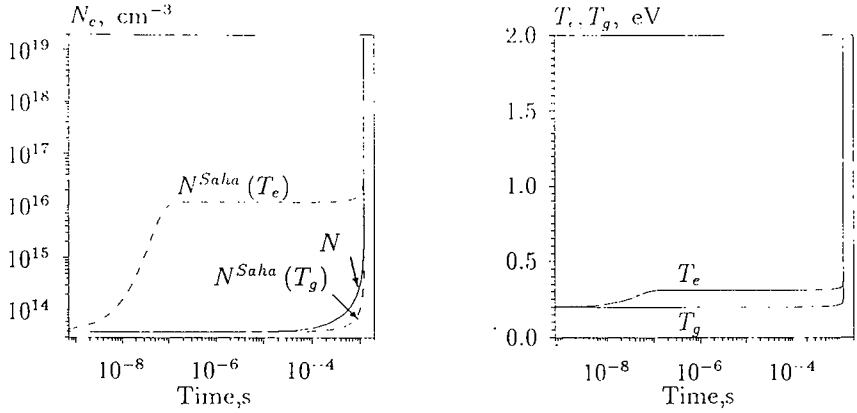

Figure 6: Optical break–down of Al vapour ($G = 10^8$ W/cm^2, initial density of vapour $6 \cdot 10^8$ cm^{-3}, initial vapour temperature 0.2 eV): concentration of charged particles ($N_e \sim \sum_{i,z} N_i^z$), temperatures of electrons T_e and ions T_g. Dashed curves: equilibrium concentrations of charged particles (based on Saha equations) for T_e, T_g temperatures.

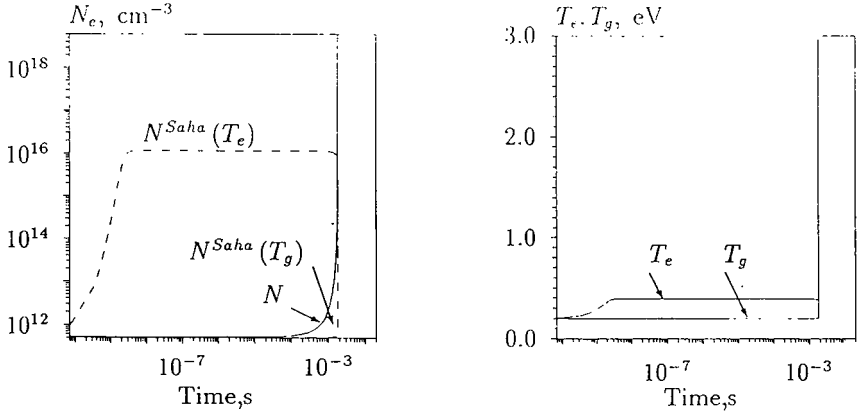

Figure 7: Optical break–down of Cu vapour ($G = 5 \cdot 10^9$ W/cm^2, initial density of vapour $6 \cdot 10^{18}$ cm^{-3}, initial vapour temperature 0.2 eV): concentration of charged particles ($N_e \sim \sum_{i,z} N_i^z$), temperatures of electrons T_e and ions T_g. Dashed curves: equilibrium concentrations of charged particles (based on Saha equations)for T_e, T_g temperatures.